

# Optical and Scintillation Properties of Ce-doped 20CsCl–20SrCl<sub>2</sub>–60ZnCl<sub>2</sub> Glasses

Daisuke Nakauchi,<sup>1\*</sup> Hiromi Kimura,<sup>2</sup> Daiki Shiratori,<sup>3</sup>  
Takumi Kato,<sup>1</sup> Noriaki Kawaguchi,<sup>1</sup> and Takayuki Yanagida<sup>1</sup>

<sup>1</sup>Nara Institute of Science and Technology (NAIST), 8916-5 Takayama, Ikoma, Nara 630-0192, Japan

<sup>2</sup>National Institute of Advanced Industrial Science and Technology,  
1-1-1 Umezono, Tsukuba, Ibaraki 305-8568, Japan

<sup>3</sup>Tokyo University of Science, 6-3-1 Nijuku, Katsushika, Tokyo 125-8585, Japan

(Received October 30, 2023; accepted January 17, 2024)

**Keywords:** scintillator, phosphor, photoluminescence, radioluminescence, afterglow

Ce-doped 20CsCl–20SrCl<sub>2</sub>–60ZnCl<sub>2</sub> glasses were investigated for their optical and scintillation properties. Under X-ray irradiation, a broad emission peak at approximately 350 nm with a shoulder peak at 375 nm was observed, and its origin was attributed to Ce<sup>3+</sup>. In the pulse height spectrum under <sup>241</sup>Am  $\alpha$ -ray, the glass doped with 0.05% Ce exhibited the highest light yield (*LY*) of 25 ph/MeV (138 ph/5.5MeV- $\alpha$ ) among zinc-halide-based glasses. The afterglow levels of the samples were superior to that of commercial CsI:Tl.

## 1. Introduction

A scintillator is a type of phosphor with the function of converting absorbed radiation energy to low-energy photons. The combination of a scintillator and a photodetector has been utilized as a scintillation detector in radiation detection, such as medicine,<sup>(1)</sup> security,<sup>(2)</sup> and resource survey.<sup>(3)</sup> In general, a scintillator requires various properties, including high light yield (*LY*), short decay, suitable effective atomic number ( $Z_{\text{eff}}$ ), and low afterglow.<sup>(4–6)</sup> Although single crystal scintillators have been mainly studied for these applications,<sup>(7–13)</sup> glass forms have various industrial advantages such as low production cost, mechanical strength, and high moldability in comparison with single crystal and ceramic forms.<sup>(13–16)</sup> However, only <sup>6</sup>Li glass (GS20) has been practically used for measuring neutrons.<sup>(17–21)</sup> Efficient X-ray and  $\gamma$ -ray measurements require glass scintillators to contain heavy elements.

To date, various glasses have been studied for scintillator applications: borate,<sup>(22)</sup> silicate,<sup>(23)</sup> phosphate,<sup>(24,25)</sup> tellurite,<sup>(26)</sup> and oxyfluoride glasses.<sup>(27)</sup> Among them, halide-based glasses have been studied for X-ray and  $\gamma$ -ray detection owing to their advantages such as low phonon energy. Zinc halides are able to form a glass matrix by themselves, and the phonon energy is lower than those of oxide- or fluoride-based glasses. Thus far, rare-earth-doped ZnCl<sub>2</sub>-based glasses have attracted attention for phosphor uses.<sup>(28–35)</sup> In our previous works, we studied 20CsCl-20BaCl<sub>2</sub>-

---

\*Corresponding author: e-mail: [nakauchi@ms.naist.jp](mailto:nakauchi@ms.naist.jp)  
<https://doi.org/10.18494/SAM4750>

$60\text{ZnCl}_2$ <sup>(36,37)</sup> and  $20\text{CsBr}-20\text{BaBr}_2-60\text{ZnBr}_2$ <sup>(38,39)</sup> glasses for radiation measurements owing to their  $Z_{\text{eff}}$  (42–43) being larger than that of GS20 ( $Z_{\text{eff}}\sim 25.5$ ), and the Ce-doped ones enabled energy distribution measurements using a radioisotope. To confirm the change trend of scintillation properties depending on alkaline earth cations, Ce-doped  $20\text{CsCl}-20\text{SrCl}_2-60\text{ZnCl}_2$  (CSZ) glasses ( $Z_{\text{eff}}\sim 38.3$ ) were investigated for optical and scintillation measurements.

## 2. Data, Materials, and Methods

$20\text{CsCl}-20\text{SrCl}_2-60\text{ZnCl}_2$  glasses doped with 0.05, 0.1, 0.5, 1.0, and 3.0% Ce were prepared by the melt quenching method.  $\text{CsCl}$  (4N),  $\text{SrCl}_2$  (4N),  $\text{ZnCl}_2$  (4N), and  $\text{CeCl}_3\cdot 6\text{H}_2\text{O}$  (4N) were used as raw powders. They were dried in vacuum at 200 °C for 1 h in a quartz tube and then enclosed using a gas burner.<sup>(40)</sup> After the powders were heated for 1 h at 700 °C using an electric furnace, the sealed ampule was dropped into water at room temperature to rapidly cool. To confirm an amorphous phase, powder X-ray diffraction (XRD) analysis was performed using MiniFlex-600, Rigaku. To measure the photoluminescence (PL) spectra and  $QY$ , Quantaaurus-QY C11347 (Hamamatsu Photonics) was used. X-ray-induced radioluminescence (XRL) spectra, kinetic decay, afterglow, and pulse height were evaluated using our laboratory-made setup.<sup>(41,42)</sup>

## 3. Results and Discussion

The prepared samples after polishing are shown in Fig. 1, and no significant differences in appearance are observed for all the samples. The samples have a cloudy and colorless appearance, which is due to the rapid deliquescence of their surface. To confirm that the samples are amorphous, the XRD patterns were evaluated as shown in Fig. 1. In all the samples, broad signals peaking at 12 and 20 degrees are observed. This halo peak suggests the formation of a glass matrix. In addition, no crystalline phase is observed at the detection limit in the XRD

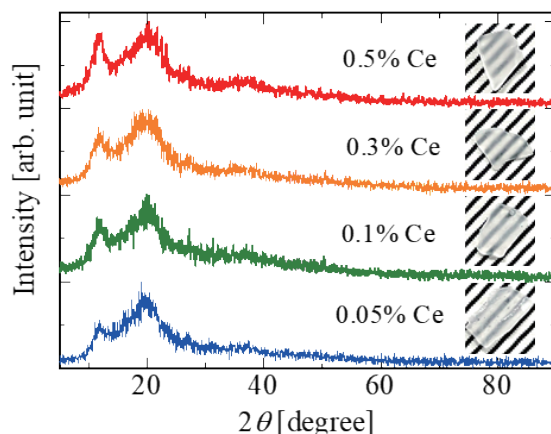


Fig. 1. (Color online) XRD patterns of CSZ glasses.

measurements. PL spectra are measured to reveal general phosphor properties. All the samples show similar spectral features, and Fig. 2 shows the spectrum of the 0.05% Ce-doped sample as a representative spectrum. The sample shows a broad emission band peaking at 370 nm, which is almost the same emission wavelength as those of past zinc-halide-based glasses.<sup>(37,38)</sup> The  $QY$  values under excitation at 320 nm are 88.1% for the 0.05% Ce-doped sample, 89.4% for the 0.1% Ce-doped sample, 85.2% for the 0.3% Ce-doped sample, and 81.9% for the 0.5% Ce-doped sample, and  $QY$  increases up to the optimal concentration (0.05%) and decreases at higher concentrations.

Figure 3 shows the XRL spectra of the samples. Similar to PL, all the samples show a broad emission peak peaking at  $\sim 370$  nm. As the Ce concentration increases, the absorption near 350 nm increases, and the spectral features indicate a peak shift; the results are consistent with the PL spectra. To confirm the response speed as a scintillator, XRL decay curves were evaluated as shown in Fig. 4. The least squares approximation shows that the decay curves have two components. The obtained decay values are close to those of zinc-halide-based glasses reported in previous studies, and this result is attributed to the 5d–4f transitions of Ce. The decay time tends to increase with the Ce concentration, and this tendency is also the same as those of other zinc-halide-based glasses.

The pulse height spectra under  $^{241}\text{Am}$   $\alpha$ -ray irradiation measured using the prepared samples and reference GS20 (1255 ph/MeV under  $\alpha$ -ray<sup>(24)</sup>) are shown in Fig. 5. In all the samples, a clear full energy peak of  $\alpha$ -rays (5.5 MeV) is observed, and the calculated LYs are approximately 22 ph/MeV for 0.05%, 21 ph/MeV for 0.1%, 25 ph/MeV for 0.3%, and 24 ph/MeV for 0.5% doped samples. These LYs are slightly higher than those of the other zinc-halide-based glasses ( $\sim 23$  ph/MeV in Ce-doped  $\text{CsCl–BaCl}_2\text{–ZnCl}_2$ <sup>(37)</sup> and  $\sim 7$  ph/MeV in Ce-doped  $\text{CsBr–SrBr}_2\text{–ZnBr}_2$ <sup>(38)</sup>).

Figure 6 shows the afterglow profiles observed after 2 ms X-ray irradiation. To compare

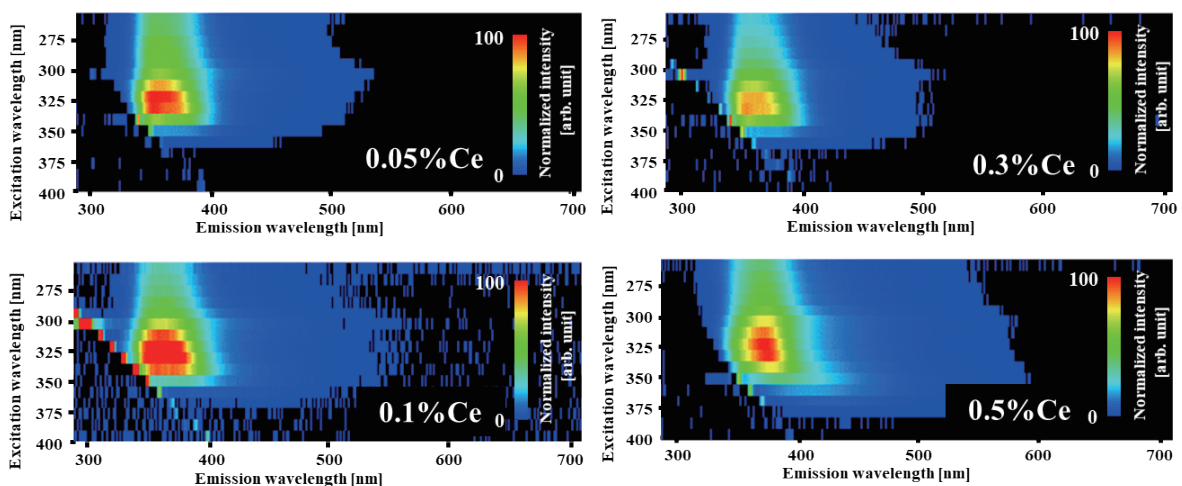


Fig. 2. (Color online) PL contour maps of CSZ glasses.

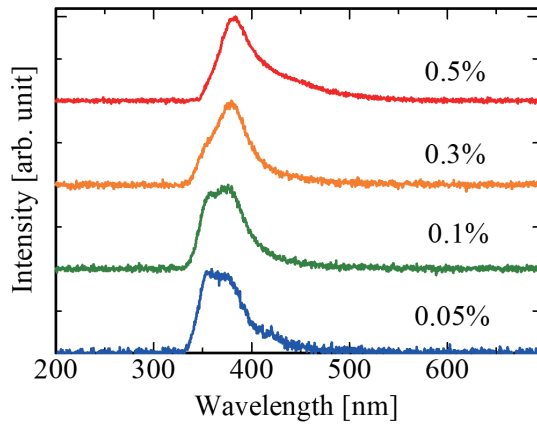


Fig. 3. (Color online) XRL spectra of CSZ glasses.

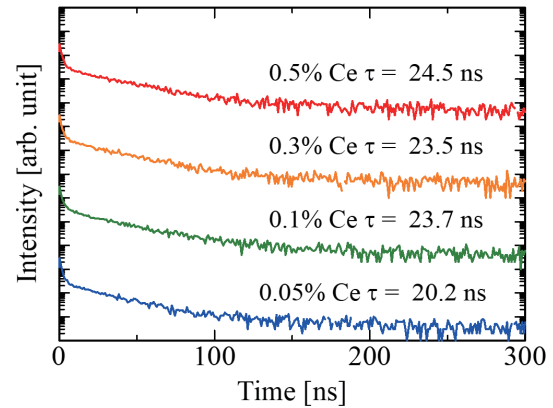


Fig. 4. (Color online) XRL decay curves of CSZ glasses.

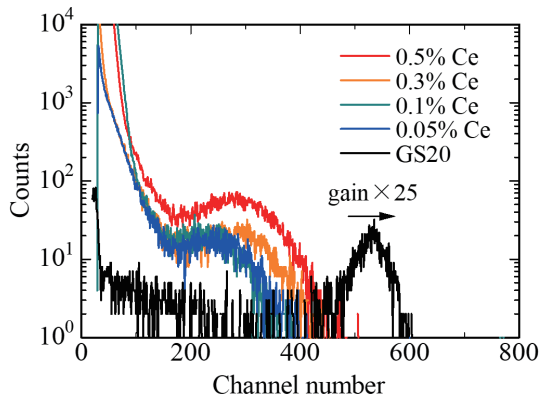


Fig. 5. (Color online) Pulse height spectra of  $^{241}\text{Am}$   $\alpha$ -rays measured using CSZ glasses.

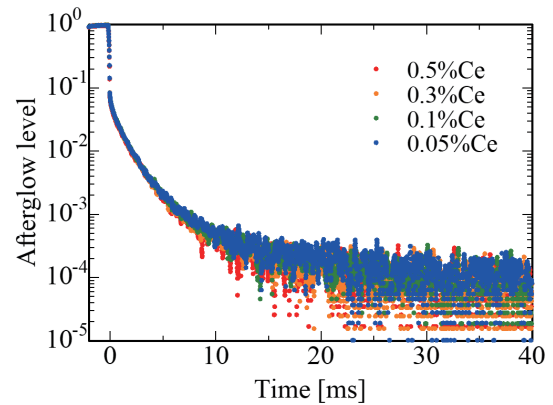


Fig. 6. (Color online) X-ray-induced afterglow curves of CSZ glasses.

afterglow levels, the afterglow level at 20 ms after X-ray irradiation was stopped ( $\text{AG}_{20\text{ms}}$ ) was defined in the same manner as in the previous papers.<sup>(43,44)</sup> The afterglow levels of the 0.05, 0.1, 0.3, and 0.5% Ce-doped glasses are respectively 245, 230, 138, and 233 ppm, which are slightly superior to that of commercial CsI:TI ( $\sim 300$  ppm<sup>(44)</sup>) and higher than that of Ce-doped CsCl-BaCl<sub>2</sub>-ZnCl<sub>2</sub> glasses ( $\sim 60$  ppm).<sup>(37)</sup>

#### 4. Conclusions

Ce-doped 20CsCl–20SrCl<sub>2</sub>–60ZnCl<sub>2</sub> glasses were synthesized to evaluate their scintillation properties. Under UV light or X-ray irradiation, the prepared glasses showed a broad emission band peaking at 370 nm, and peak positions slightly redshifted with increasing Ce concentration. XRL decay curves showed that decay time constants are approximately 20–30 ns, which are

reasonable for the 5d–4f emission of Ce. In the pulse height spectra under  $^{241}\text{Am}$   $\alpha$ -ray irradiation, a full energy peak was observed in all the samples, and the 0.3% doped sample showed the highest LY of 25 ph/MeV (138 ph/5.5MeV- $\alpha$ ) under  $\alpha$ -rays among the samples. The  $\text{AG}_{20\text{ms}}$  values of the samples were approximately 100–300 ppm, which were superior to those of commercial CsI:TI scintillators. Considered comprehensively from LY and  $\text{AG}_{20\text{ms}}$ , the 0.3% Ce-doped glass is the most suitable for scintillator uses among the present glasses. The obtained samples were superior to all reported zinc-halide-based glasses, but were inferior to practical GS20 except for  $Z_{\text{eff}}$  and  $QY$ . Some zinc-halide-based glasses exhibit higher  $QY$ s than GS20 but lower LYs than GS20. The cause is considered to be the low energy transport efficiency despite the low phonon energy, but the actual cause is unclear at present. The development of halide glasses to overcome this problem is expected.

### Acknowledgments

This work was supported by Grants-in-Aid for Scientific Research A (22H00309), Scientific Research B (22H03872, 22H02939, 21H03733, and 21H03736), Early-Career Scientists (23K13689), and Challenging Exploratory Research (22K18997) from JSPS. The Cooperative Research Project of the Research Center for Biomedical Engineering, A-STEP from JST, Kazuchika Okura Memorial Foundation, Asahi Glass Foundation, Nakatani Foundation, and Konica Minolta Science and Technology Foundation are also acknowledged.

### References

- 1 C. W. E. van Eijk: *Phys. Med. Biol.* **47** (2002) R85. <https://doi.org/10.1088/0031-9155/47/8/201>
- 2 Q. Liu, Y. Cheng, Y. Yang, Y. Peng, H. Li, Y. Xiong, and T. Zhu: *Appl. Radiat. Isot.* **163** (2020) 109217. <https://doi.org/10.1016/j.apradiso.2020.109217>
- 3 C. L. Melcher: *Nucl. Instrum. Methods Phys. Res., B* **40–41** (1989) 1214. [https://doi.org/10.1016/0168-583X\(89\)90622-8](https://doi.org/10.1016/0168-583X(89)90622-8)
- 4 C. W. E. van Eijk: *Nucl. Instrum. Methods Phys. Res., A* **392** (1997) 285. [https://doi.org/10.1016/S0168-9002\(97\)00239-8](https://doi.org/10.1016/S0168-9002(97)00239-8)
- 5 S. E. Derenzo, M. J. Weber, E. Bourret-Courchesne, and M. K. Klintonberg: *Nucl. Instrum. Methods Phys. Res., A* **505** (2003) 111. [https://doi.org/10.1016/S0168-9002\(03\)01031-3](https://doi.org/10.1016/S0168-9002(03)01031-3)
- 6 P. Dorenbos: *Directions in Scintillation Materials Research*, in: *Radiat. Detect. Med. Appl.* (Springer Netherlands) pp. 191–207. [https://doi.org/10.1007/1-4020-5093-3\\_8](https://doi.org/10.1007/1-4020-5093-3_8)
- 7 H. Fukushima, D. Nakauchi, T. Kato, N. Kawaguchi, and T. Yanagida: *Sens. Mater.* **35** (2023) 429. <https://doi.org/10.18494/SAM4139>
- 8 D. Shiratori, H. Fukushima, D. Nakauchi, T. Kato, N. Kawaguchi, and T. Yanagida: *Sens. Mater.* **35** (2023) 439. <https://doi.org/10.18494/SAM4140>
- 9 P. Kantuptim, T. Kato, D. Nakauchi, N. Kawaguchi, K. Watanabe, and T. Yanagida: *Sens. Mater.* **35** (2023) 451. <https://doi.org/10.18494/SAM4141>
- 10 K. Okazaki, D. Nakauchi, H. Fukushima, T. Kato, N. Kawaguchi, and T. Yanagida: *Sens. Mater.* **35** (2023) 459. <https://doi.org/10.18494/SAM4144>
- 11 D. Nakauchi, H. Fukushima, T. Kato, N. Kawaguchi, and T. Yanagida: *Sens. Mater.* **34** (2022) 611. <https://doi.org/10.18494/SAM3696>
- 12 Y. Fujimoto, D. Nakauchi, T. Yanagida, M. Koshimizu, and K. Asai: *Sens. Mater.* **34** (2022) 629. <https://doi.org/10.18494/SAM3693>
- 13 D. Nakauchi, F. Nakamura, T. Kato, N. Kawaguchi, and T. Yanagida: *Sens. Mater.* **35** (2023) 467. <https://doi.org/10.18494/SAM4138>
- 14 T. Kunikata, T. Kato, D. Shiratori, P. Kantuptim, D. Nakauchi, N. Kawaguchi, and T. Yanagida: *Sens. Mater.* **35** (2023) 491. <https://doi.org/10.18494/SAM4145>

- 15 M. Koshimizu, Y. Fujimoto, and K. Asai: *Sens. Mater.* **35** (2023) 521. <https://doi.org/10.18494/SAM4149>
- 16 S. Matsumoto, T. Watanabe, and A. Ito: *Sens. Mater.* **34** (2022) 669. <https://doi.org/10.18494/SAM3698>
- 17 Y. Zou, W. Zhang, C. Li, Y. Liu, and H. Luo: *Radiat. Meas.* **127** (2019) 106148. <https://doi.org/10.1016/j.radmeas.2019.106148>
- 18 N. Pu, T. Nishitani, T. Tanaka, and M. Isobe: *Fusion Eng. Des.* **151** (2020) 111418. <https://doi.org/10.1016/j.fusengdes.2019.111418>
- 19 S. Kumar, M. Herzkamp, D. Durini, H. Nöldgen, and S. van Waasen: *Nucl. Instrum. Methods Phys. Res., A* **954** (2020) 161697. <https://doi.org/10.1016/j.nima.2018.12.012>
- 20 Y. Oshima, K. Watanabe, H. Shiga, and G. Wakabayashi: *Sens. Mater.* **35** (2023) 545. <https://doi.org/10.18494/SAM4148>
- 21 T. Fujiwara, K. Kino, N. Oshima, and M. Furusaka: *Sens. Mater.* **35** (2023) 537. <https://doi.org/10.18494/SAM4147>
- 22 D. Nakauchi, G. Okada, Y. Fujimoto, N. Kawano, N. Kawaguchi, and T. Yanagida: *Opt. Mater.* **72** (2017) 190. <https://doi.org/10.1016/j.optmat.2017.05.063>
- 23 N. Kawaguchi, K. Watanabe, D. Shiratori, T. Kato, D. Nakauchi, and T. Yanagida: *Sens. Mater.* **35** (2023) 499. <https://doi.org/10.18494/SAM4136>
- 24 M. Akatsuka, K. Shinozaki, D. Nakauchi, T. Kato, G. Okada, N. Kawaguchi, and T. Yanagida: *Opt. Mater.* **94** (2019) 86. <https://doi.org/10.1016/j.optmat.2019.04.064>
- 25 N. Kawaguchi, D. Nakauchi, T. Kato, Y. Futami, and T. Yanagida: *Sens. Mater.* **34** (2022) 725. <https://doi.org/10.18494/SAM3705>
- 26 R. Nakamori, N. Kawano, A. Takaku, D. Onoda, Y. Takebuchi, H. Fukushima, T. Kato, K. Shinozaki, and T. Yanagida: *Sens. Mater.* **34** (2022) 707. <https://doi.org/10.18494/SAM3689>
- 27 K. Shinozaki, S. Sukenaga, H. Shibata, and T. Akai: *J. Am. Ceram. Soc.* **102** (2019) 2531. <https://doi.org/10.1111/jace.16165>
- 28 T. Tsuneoka, K. Kojima, and S. Bojja: *J. Non. Cryst. Solids* **202** (1996) 297. [https://doi.org/10.1016/0022-3093\(96\)00196-2](https://doi.org/10.1016/0022-3093(96)00196-2)
- 29 J. Qiu, K. Kojima, A. Kubo, M. Yamashita, and K. Hirao: *Phys. Chem. Glasses* **41** (2000) 150.
- 30 M. Shojiya, Y. Kawamoto, and K. Kadono: *J. Appl. Phys.* **89** (2001) 4944. <https://doi.org/10.1063/1.1337586>
- 31 T. Kishimoto, N. Wada, and K. Kojima: *Phys. Chem. Glasses* **43** (2002) 233.
- 32 M. Shojiya, M. Takahashi, R. Kanno, Y. Kawamoto, and K. Kadono: *J. Appl. Phys.* **82** (1997) 6259. <https://doi.org/10.1063/1.366545>
- 33 B. Dussardier, J. Wang, D. C. Hanna, and D. N. Payne: *Opt. Mater.* **4** (1995) 565. [https://doi.org/10.1016/0925-3467\(95\)00008-9](https://doi.org/10.1016/0925-3467(95)00008-9)
- 34 S. Zhao, Z. Xu, L. Wang, and S. Wageh: *Sci. China Phys., Mech. Astron.* **53** (2010) 310. <https://doi.org/10.1007/s11433-010-0117-y>
- 35 G. Ito, H. Kimura, D. Shiratori, D. Nakauchi, T. Kato, N. Kawaguchi, and T. Yanagida: *Sens. Mater.* **34** (2022) 685. <https://doi.org/10.18494/SAM3681>
- 36 G. Ito, H. Kimura, D. Shiratori, K. Hashimoto, D. Nakauchi, M. Koshimizu, T. Kato, N. Kawaguchi, and T. Yanagida: *J. Mater. Sci. Mater. Electron.* **32** (2021) 8725. <https://doi.org/10.1007/s10854-021-05544-y>
- 37 G. Ito, H. Kimura, D. Shiratori, D. Nakauchi, T. Kato, N. Kawaguchi, and T. Yanagida: *Optik* **226** (2021) 165825. <https://doi.org/10.1016/j.ijleo.2020.165825>
- 38 H. Kimura, T. Fujiwara, M. Tanaka, T. Kato, D. Nakauchi, N. Kawaguchi, and T. Yanagida: *Sens. Mater.* **35** (2023) 513. <https://doi.org/10.18494/SAM4146>
- 39 H. Kimura, T. Kato, D. Nakauchi, N. Kawaguchi, and T. Yanagida: *Sens. Mater.* **34** (2022) 691. <https://doi.org/10.18494/SAM3687>
- 40 D. Nakauchi, Y. Fujimoto, T. Kato, N. Kawaguchi, and T. Yanagida: *Jpn. J. Appl. Phys.* **60** (2021) 092002. <https://doi.org/10.35848/1347-4065/ac15af>
- 41 T. Yanagida, K. Kamada, Y. Fujimoto, H. Yagi, and T. Yanagitani: *Opt. Mater.* **35** (2013) 2480. <https://doi.org/10.1016/j.optmat.2013.07.002>
- 42 T. Yanagida, Y. Fujimoto, T. Ito, K. Uchiyama, and K. Mori: *Appl. Phys. Express* **7** (2014) 062401. <https://doi.org/10.7567/APEX.7.062401>
- 43 N. G. Starzhinskiy, O. T. Sidletskiy, G. Tamulaitis, K. A. Katrunov, I. M. Zenya, Y. V. Malyukin, O. V. Viagin, A. A. Masalov, and I. A. Rybalko: *IEEE Trans. Nucl. Sci.* **60** (2013) 1427. <https://doi.org/10.1109/TNS.2013.2244910>
- 44 D. Nakauchi, T. Kato, N. Kawaguchi, and T. Yanagida: *Appl. Phys. Express* **13** (2020) 122001. <https://doi.org/10.35848/1882-0786/abc574>